

A Study on the Helical Flow of Newtonian and Non-Newtonian Fluid

Nam-Sub Woo, Young-Kyu Hwang[†], Young-Ju Kim^{*}

Department of Mechanical Eng., Sungkyunkwan University, Suwon 440-746, Korea

**Fluid Eng. & Deep-Sea Mining, Korea Institute of Geoscience & Mineral Resources, Daejeon 305-350, Korea*

Key words: Helical flow, Skin friction coefficient, Eccentric annulus, Non-Newtonian fluid

ABSTRACT: This study concerns the characteristics of helical flow in a concentric and eccentric annulus with a diameter ratio of 0.52 and 0.9, whose outer cylinders are stationary and inner ones are rotating. Pressure losses and skin friction coefficients have been measured for fully developed flows of water and 0.2% aqueous of sodium carboxymethyl cellulose (CMC), respectively, when the inner cylinder rotates at the speed of 0~500 rpm. The effect of rotation on the skin friction is significantly dependent on the flow regime. In all flow regimes, the skin friction coefficient is increased by the inner cylinder rotation. The change of skin friction coefficient corresponding to the variation of rotating speed is large for the laminar flow regime, whereas it becomes smaller as Re increases for the transitional flow regime and, then, it gradually approach to zero for the turbulent flow regime.

Nomenclature

C_f	: skin friction coefficient
D_h	: hydraulic diameter, $2(R_2 - R_1)$
dp/dz	: axial pressure loss [Pa/m]
e	: offset from center [mm]
h	: head [mm]
K	: consistency factor
N	: rotational speed [rpm]
n	: flow behavior index
R_1	: radius of inner cylinder [mm]
R_2	: radius of outer cylinder [mm]
Re	: axial Reynolds number, $\overline{v_z}^{2-n} D_h^n / \nu$
v_z	: axial bulk velocity [m/s]
Δz	: distance between tap [mm]

δ	: annular gap, $R_2 - R_1$ [mm]
ϵ	: eccentricity, e/δ
μ	: viscosity [Pa·s]
ρ	: density [kg/m ³]
τ	: shear stress [Pa]
Φ	: radius ratio, R_1/R_2

Superscripts

-	: average value
---	-----------------

Subscripts

c	: critical value
h	: hydraulic

Greek symbols

γ	: shear strain rate [s ⁻¹]
----------	--

1. Introduction

Annular flow refers to the flow of fluids through an annular space between two infinitely long circular tubes. If one of the tubes is rotating, the fluid elements will flow through the annulus following a helical path. This is so

[†] Corresponding author

Tel.: +82-31-290-7437; fax: +82-31-290-5889

E-mail address: kyjp@skku.edu

called annular helical flow and it occurs in many engineering operations such as the flow of drilling fluids through an annulus when the drill pipe is rotating.

Drilling with high speed pipe rotation requires excellent lateral stability for the pipe in order to avoid destructive vibrations. One means of providing this lateral stability is a narrow gap around the pipe. Small vibration in annular gap, well bore eccentricity, and pipe rotational speed strongly affect pressure loss of fluid flowing in the narrow annulus of a slim hole well.

These factors, usually negligible in conventional drilling, significantly increase the difficulty of calculating and controlling pressure during slim hole drilling. Accurate calculations of pressure loss in the well bore are necessary to control the well, optimize bit hydraulics, and avoid excessive pressure. And it is more difficult in a slim hole drilling than in a conventional drilling.

It is well known that the stability of a viscous flow in a small annular gap between concentric cylinders with rotation of the inner one was first considered experimentally and theoretically by Taylor.⁽¹⁾ He also found that the flow is stable when the inner cylinder is stationary and the outer one is rotating. Conversely, if the outer cylinder is stationary, the flow becomes unstable.

Recently, Nouri and Whitelaw⁽²⁾ showed that the value of critical axial Reynolds number Re_c in a rotating annulus decreases as both the rotational Reynolds number Re_w and the ratio of eccentricity increases. Escudier and Gouldson⁽³⁾ investigated the influence of rotation on the axial velocity distribution and found that it is most apparent at low bulk flow Reynolds number. Delwiche et al.⁽⁴⁾ showed that the variations of annular gap, well bore eccentricity and shaft rotational speed have strong effect on the pressure loss of fluid flowing in a narrow annulus of slim hole drilling. Due to these factors, it is very difficult to calculate accurately

and control pressures losses in slim hole well bores.

Siginer and Bakhtiyarov⁽⁵⁾ carried out an analytical and experimental study on the flow of glycerol/water mixture and oil field spacer fluid in an eccentric annulus. Escudier et al.⁽⁶⁾ presented numerical results for the flow of a shear-thinning power law fluid through an eccentric annulus. They also summarized the literature of investigations of laminar flow of non-Newtonian fluids through annular channels.

However, attempts to model non-Newtonian fluid flow in slim hole annuli with high speed pipe rotation have been hampered by the lack of quality data. So, this study concerns an experimental and numerical study of fully developed laminar flows of Newtonian and non-Newtonian fluids through concentric and eccentric slim hole annuli with combined bulk axial flow and inner cylinder rotation.

In an experimental study, pressure losses and skin friction coefficients through the rotating annulus with diameter ratios of 0.52 and 0.9 have been measured in a concentric annulus using water and 0.2% CMC aqueous solution. According to Nouri and Whitelaw,⁽²⁾ maximum drag reduction of CMC solutions has been achieved with the 0.2% CMC solution. So there seems little advantage in solutions of polymer concentrations greater than 0.2% CMC solution if the reason for their use is associated with shear-thinning. The rotational speed of inner cylinder is between 0 and 500 rpm. The axial bulk flow Reynolds number is in range of $100 < Re < 20,000$.

In a numerical study, flow pattern and shear stress of water in an eccentric annulus are calculated. The effect of shaft rotation, radius ratio, eccentricity, flow rate on the skin friction coefficient and shear stress are investigated.

2. Data reduction

The equation of the average axial velocity in

a concentric annulus without the rotation can be expressed in terms of the pressure loss dp/dz as follows (Bird et al.⁽⁷⁾),

$$\frac{dp}{dz} = \frac{gh \sin \theta (\rho_{ccl4} - \rho)}{\Delta z} \quad (1)$$

where ρ , ρ_{ccl4} , h and Δz denote the density of the fluid, the density of *ccl4*, the difference of head of the manometer, and the distance between pressure holes, respectively. Also, the skin friction coefficient C_f can be obtained as Eq. (2),

$$C_f = \frac{dp}{dz} \frac{D_h}{2\rho v^2} \quad (2)$$

where, $D_h = 2(R_2 - R_1)$ is the hydraulic diameter.

2.1 Properties of working fluid

Non-Newtonian fluids are those for which the strain rate and stress curve are not linear, i.e., the viscosity of non-Newtonian fluids is not constant at a given temperature and pressure but depends on other factors such as the rate of shear in the fluid, the apparatus in which the fluid is contained or even the previous history of the fluid. Consequently, the determination of the shear stress-shear rate curve must be an initial consideration.

Mud characteristics are very important parameters to know for accurate predictions of pressure loss when the annular clearances are thin. In the case of 0.2% CMC solution, the flow behavior index n is smaller than one and the power law relating the shear stress τ to the shear rate γ is given by

$$\tau = K\gamma^n \quad (3)$$

where, n is the flow behavior index and K is the consistency factor. The value of n is the non-Newtonian degree of the fluid rheological

behavior and the K value is a measure of the consistency of the fluid. The apparent viscosity, μ_a for a power law fluid may be expressed in terms of n and K as follows,

$$\mu_a = K\gamma^{n-1} \quad (4)$$

The effective viscosity of 0.2% CMC solution is 6.5 cP and the flow behavior index, n is measured as 0.87.

3. Experimental and numerical method

3.1 Experimental apparatus and method

The experimental set-up consists of a cylindrical section, fluid-providing and rotating part and measuring part which measure the flow rate, pressure loss and the temperature as shown in Fig. 1. A flow loop was designed and constructed with a replaceable annular test section to simulate a slim hole well annulus.

A centrifugal pump delivers the working fluid from a supply tank to a surge tank. The surge tank located immediately after the pump outlet

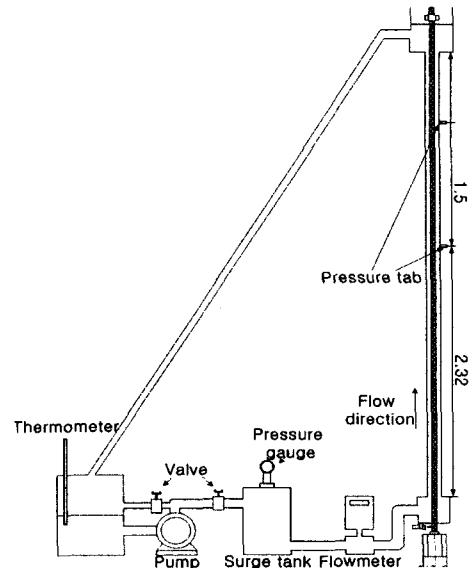


Fig. 1 Experimental set-up.

acts to remove pulsation in the flow prior to entry into the test section. The fluid flows into the annular passage with outer pipes of nominal inside diameter, D_2 , of 43 mm for diameter ratio of 0.9 and an inner stainless steel rod of diameter, D_1 , of 30 mm. To insure fully developed flow in the measuring section, the length of straight pipe upstream of the test section is 2.32 m, corresponding to 126 hydraulic diameters.

Static pressures are measured with holes of 0.5 mm diameter distributed longitudinally in the outer cylinder. Two static pressure taps are installed along the flow direction in measuring part as shown in Fig. 1. The static pressures are read from a calibrated manometer bank with 1 mm resolution. The specific gravity of the manometer fluid *ccl4* is 1.88, and it gives a height in the range of 20~600 mm.

In the experiment, the pressure losses have been measured by Eq. (5),

$$\frac{dp}{dz} = \frac{gh(\rho_{ccl4} - \rho)}{\Delta z} \quad (5)$$

The experimental values of the skin friction coefficients in a laminar regime can be evaluated by substituting Eq. (5) into Eq. (2).

The flow rate has been measured with a magnetic flow meter whose accuracy is within the limit of 0.5%. The temperature of the working fluid has been measured with a digital multi-meter. The inner cylinder may be rotated at any speed up to a maximum of 1,000 rpm by means of an A. C. motor. The temperature of the fluid within the pipe rig is maintained at $25 \pm 0.5^\circ\text{C}$.

The viscosity of 0.2% CMC solution is measured using the rotating type viscometer (Brookfield DV-III+ Programmable Rheometer).

3.2 Numerical simulation

A control volume based finite volume method is used to solve the equations of motion. The

problem reduced to the solution of the conservation of mass and momentum equations along with the appropriate boundary and initial conditions.

$$\nabla \cdot u = 0 \quad (6)$$

$$u \cdot \nabla u = -\frac{1}{\rho} \nabla p + \nu \nabla^2 u \quad (7)$$

where u , ρ , ν , p denote the velocity vector, the density, the kinetic viscosity and the pressure of fluid, respectively. For non-Newtonian fluid, viscosity model, which is explained in Eq. (4), is added to the same momentum equation.

In a numerical study, a laminar flow of water in an eccentric annulus has been calculated. A typical mesh of the discretised bore hole domain in the horizontal plain is shown in Fig. 2.

The inner cylinder radius is $R_1=10$ mm, the outer cylinder $R_2=19.2$ mm (diameter ratio of 0.52) and the eccentricity, e varied from 0.2 to 0.7.

The constant velocity of fluid and the Neumann boundary conditions are imposed on inlet and outlet of annulus, respectively. No slip boundary wall conditions are used at the inner and outer cylinders. The rotational speed of the inner cylinder is changed from 0 to 150 rpm.

Since the fully developed flow condition was of concern here, only one row of cell was

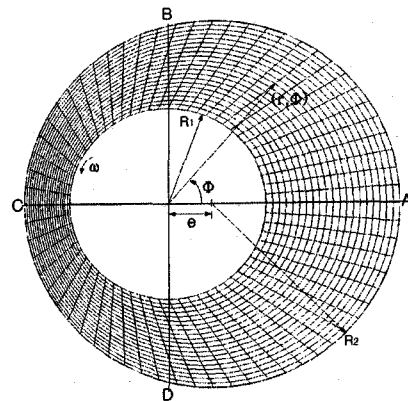


Fig. 2 Computational grid of annulus.

needed in the axial direction. That is, stream-wise fully developed periodic condition is used. The distortions of the axial velocity distribution and the movement of the peak axial velocity are calculated to understand the effects of rotation and eccentricity.

4. Results and discussion

4.1 Experimental results

Although this paper is concerned with the flow of some Newtonian and non-Newtonian fluids, the practical motivation for the work is its relevance to the flow of slim hole drilling in an oil and gas well bore during drilling operation.

In the case of water, it is difficult to measure the pressure loss accurately because it is so small for the low flow rate. However, in the case of 0.2% CMC solution, it is relatively easy to measure the pressure loss since its viscosity is larger than that of water.

The influence of the inner cylinder rotation for fluids is apparent from the skin friction coefficient versus the Reynolds number. The skin friction coefficient is obtained from pressure loss measurements by using Eq. (2).

For comparison purpose, curves representing standard friction factor correlations for fully de-

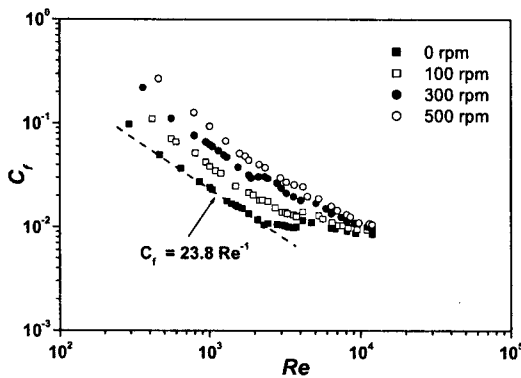
veloped laminar flow of water in a concentric annulus with radius ratio 0.52 and no rotation of the inner cylinder are shown in Fig. 3(a). The results show that the value of C_f without rotation agrees with the correlation curve ($C_f = 23.8/Re$) of Nouri and Whitelaw.⁽²⁾

In the case of water as shown in Fig. 3(a), the skin friction coefficient in non-rotating decreases linearly as the Reynolds number is increased and it increases as the radius ratios and the rotational speed of the inner cylinder are increased. The correlation between C_f-Re is $C_f = 23.8/Re$ in the radius ratio of 0.52 and the numerator approaches to 24 as the radius ratio reaches to 1.

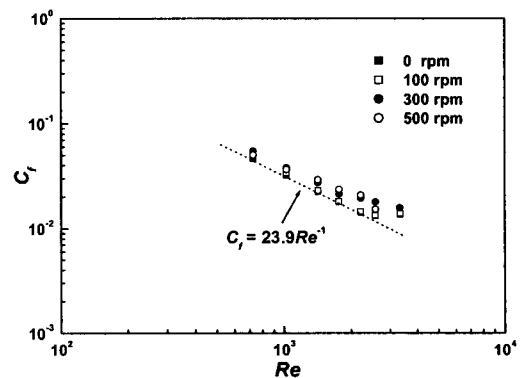
The skin friction coefficient decreases linearly as the Reynolds number is increased in laminar flow regime. The fact that the skin friction coefficient drops off with increasing the Reynolds number should not mislead us into thinking that shear stress decreases with velocity.

In the case of water when the radius ratio is 0.9, the increasing rates of the pressure loss is about 10 times for the radius ratios of 0.52 as reported by Seo et al.⁽⁸⁾ Also for the same flow rate and rotational speed, the skin friction coefficient of radius ratio, 0.52 is 2~3 times larger than that of 0.9.

The magnitude of axial velocity increases



(a) $\phi=0.52$



(b) $\phi=0.9$

Fig. 3 Skin friction coefficient of water as a function of Re at 0~500 rpm.

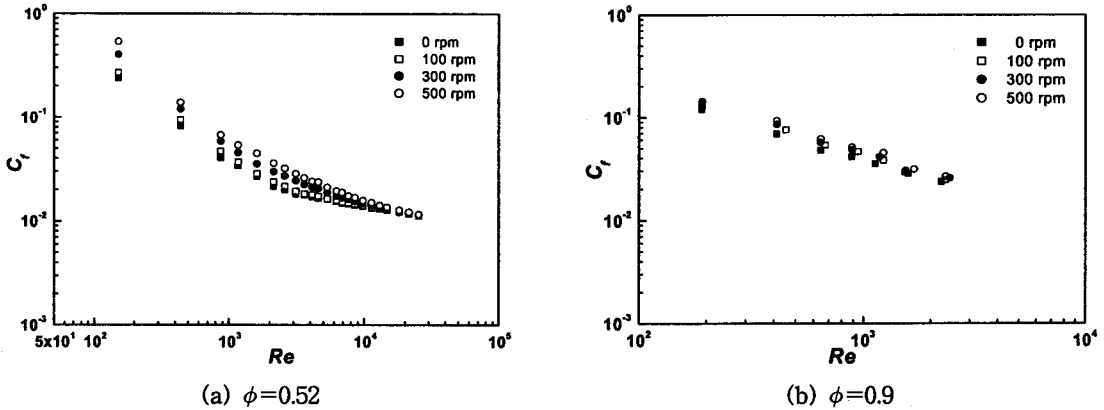


Fig. 4 Skin friction coefficient of 0.2% CMC solution as a function of Re at 0~500 rpm.

abruptly with increasing radius ratios due to the decrease of flowing area. So the effect of rotation on the skin friction coefficient becomes weak compared with axial flow rate as the radius ratios increases. There is no reliable skin friction coefficient correlation in the transitional flow regime. For turbulent flow of fluid, the skin friction coefficient decreases gradually with the Reynolds number.

For the 0.2% CMC solution, the effect of rotation is decreased noticeably compared with water for all radius ratios as shown in Fig. 4. And this is more distinguishable with increasing the radius ratio. That is, the flow behavior index n is smaller than one.

The effect of rotation of the inner cylinder on the skin friction coefficient is larger in water and it becomes weak in 0.2% CMC solution. This is because of the resistance against the flow of shear thinning fluid decreases with increasing shear rate.

That is, drag reduction with shear thinning fluids is a direct result of the thickening of the sub-layer due to the expansion of molecules with a mechanism that has been explained by Lumley.⁽⁹⁾

The maximum uncertainties in manometer reading were $\pm 5\%$ at the lowest measured flow rate and considerably less at the higher flow rate.

4.2 Numerical results

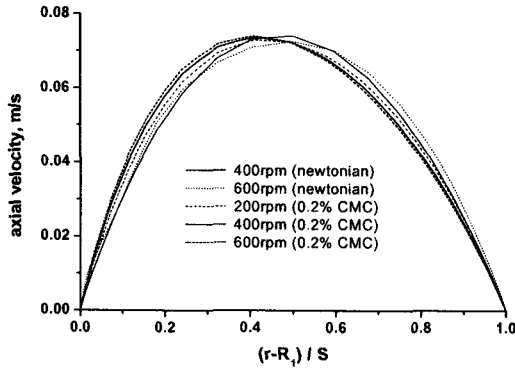
To obtain a more realistic result of the drilling operation, helical flow of water in an eccentric annulus was considered. Calculations have been extended for the case where the inner cylinder rotates about its own axis at a constant rotational speed. Detailed calculations have been carried out for radius ratio of 0.52 covering eccentricities up to 0.7 and rotational speed of inner cylinder up to 150 rpm.

To validate our numerical calculation, the skin friction coefficients obtained from experiment and numerical calculation were compared and this results were reported in a previous paper by Kim et al.⁽¹⁰⁾

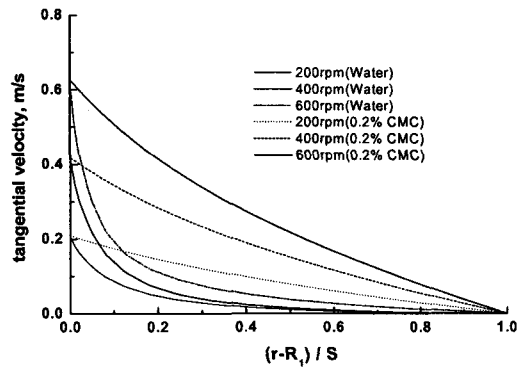
Contour of axial and tangential velocities for the water and 0.2% CMC solution covering are shown in Fig. 5.

As shown in Fig. 5(a) compared with water, the axial velocity of 0.2% CMC solution is decreased as the rotational speed of the inner cylinder is increased. And the location of the maximum velocity is shifted to the inner cylinder. This is because of the shear thinning effect of 0.2% CMC solution.

For the tangential velocities, the tangential velocity gradient is increased with the increase of the rotational speed of the inner cylinder. Also, for the same condition velocity gradient



(a) Axial velocity



(b) Tangential velocity

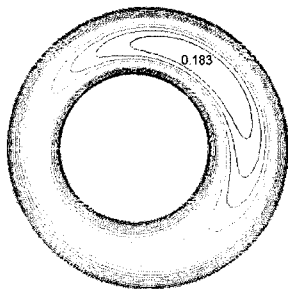
Fig. 5 Rotating flow velocities of the water and non-Newtonian fluids with axial and tangential velocity.

of water is larger than that of 0.2% CMC solution. That is, the effect of rotational speed is larger in water than in 0.2% CMC solution.

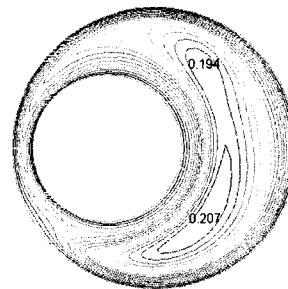
Contour of axial velocity for water covering eccentricities of 0.2, 0.5 and 0.7 are shown in

Figs.6 and 7.

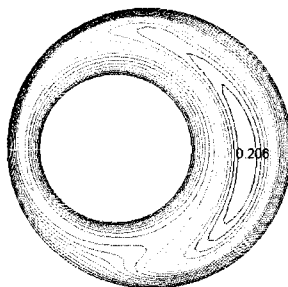
For a fixed rotation speed at low eccentricity ($\epsilon=0.2$) in Fig. 6, the tangential flow around the annulus is slightly reduced by the blockage effect associated with the eccentricity. So the



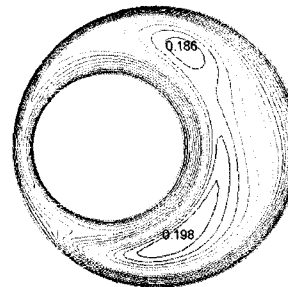
(a) $\epsilon=0.2$



(a) 100 rpm



(b) $\epsilon=0.5$



(b) 150 rpm

Fig. 6 Axial iso-velocities [m/s] for radius ratio is 0.52 and $Re=1,050$ in an eccentric annulus at 100 rpm.

Fig. 7 Axial iso-velocities [m/s] for radius ratio is 0.52 and $Re=1,050$ in an eccentricity of 0.7.

axial velocity peak is moved in the sense of rotation into a narrow gap. As the eccentricity is increased ($\varepsilon=0.5$), recirculation of the cross flow develops adjacent to the surface of the outer cylinder and the axial velocity peak is roughly centered in the wide gap as shown in Fig. 6(b).

An unexpected feature of the calculations for eccentricity of 0.7, but not seen for $\varepsilon=0.2$ and 0.5, is the appearance of a second peak in the axial velocity, located in the narrowing gap, for combinations of very high eccentricities and rotation as shown in Fig. 7. This flow pattern is also reported by Escudier et al.⁽¹¹⁾

The distortion of the axial velocity distribution and the movement of the peak axial velocity, due to the combined effects of eccentricity and rotation, result in the distributions of the surface shear stress.

5. Conclusions

In this study the effects of the rotational speeds, radius ratio, flow rates, eccentricity and working fluids on the skin friction coefficients in a concentric and an eccentric slim hole annuli have been investigated experimentally and numerically.

In the radius ratio of 0.9, the skin friction coefficients with 0.2% CMC solution increased by about 45% with rotation from 0 to 500 rpm in laminar flow. This is 20% smaller values than in the radius ratio of 0.52. That is, slim hole drilling with the shear thinning fluids is attractive in controlling pressure loss.

A numerical analysis considered mainly the effects of annular eccentricity and inner cylinder rotation. The present analysis has demonstrated the importance of the drill pipe rotation and eccentricity. In eccentricity of 0.7, the flow field is recirculation dominated and unexpected behavior is observed. For high rotational speed of inner cylinder, the axial velocity peak is so strongly advected towards the lower side of the

inner cylinder, where it generates a strong rotation directed layer, that two opposing effects act to create two local peaks of the axial velocity.

Acknowledgement

This work was supported by the Brain Korea 21 Project in 2007 and the Korea Institute of Geoscience and Mineral Resources.

References

1. Taylor, G. I., 1923, Stability of a viscous fluid contained between two rotating cylinders, *Phil. Trans. A*, Vol. 223, pp. 289-343.
2. Nouri, J. M. and Whitelaw, J. H., 1994, Flow of Newtonian and non-Newtonian fluids in a concentric annulus with rotation of the inner cylinder, *J. Fluids Eng.*, Vol. 116, pp. 821-827.
3. Escudier, M. P. and Gouldson, I. W., 1995, Concentric annular flow with centerbody rotation of a Newtonian and a shear-thinning liquid, *Int. J. Heat and Fluid Flow*, Vol. 16, pp. 156-162.
4. Delwiche, R. A., Lejeune, M. W. D. and Stratabit, D. B., 1992, Slimhole drilling hydraulics, Society of Petroleum Engineers Inc., SPE 24596, pp. 521-541.
5. Siginer, D. A. and Bakhtiyarov, S. I., 1998, Flow of drilling fluids in eccentric annuli, *J. Non-Newtonian Fluid Mech.*, Vol. 78, pp. 119-132.
6. Escudier, M. P., Oliveira, P. J. and Pinho, F. T., 2002, Fully developed laminar flow of purely viscous non-Newtonian liquids through annuli, including the Effects of Eccentricity and Inner-Cylinder Rotation, *I. J. Heat and Fluid Flow*, Vol. 23, pp. 52-73.
7. Bird, R. B., Lightfoot, E. N. and Stewart, W. E., 1960, *Transport Phenomena*, pp. 34-70.
8. Seo, B. T., Woo, N. S. and Hwang, Y. K., 2006, A study on the flow of drilling fluids

- in slim hole annuli, *Korean Journal of Air-Conditioning and Refrigeration Engineering*, Vol. 18, No. 4, pp. 370-376.
9. Lumley, J.L., 1977, Drag reduction in two phase and polymer flows, *The Physics of Fluids*, Vol. 20, pp. 64-71.
 10. Kim, Y. J., Hwang Y. K. and Woo, N. S., 2002, A study on the transitional flows in a concentric annulus with rotating inner cylinder, *Korean Journal of Air-Conditioning and Refrigeration Engineering*, Vol. 14, No. 10, pp. 833-843.
 11. Escudier, M. P., Gouldson, I. W., Oliveira, P. J. and Pinho, F. T., 2000, Effects of inner cylinder rotation on laminar flow of a Newtonian fluid through an eccentric annulus, *I. J. Heat and Fluid Flow*, Vol. 21, pp. 92-103.